

# A multi-functionalized montmorillonite for co-operative catalysis in one-pot Henry reaction and water pollution remediation

Cite this: *J. Mater. Chem. A*, 2014, 2, 7526

G. Bishwa Bidita Varadwaj,<sup>ab</sup> Surjyakanta Rana,<sup>a</sup> Kulamani Parida<sup>\*ab</sup> and Binod Bihari Nayak<sup>c</sup>

The present work provides a simple approach for the surface modification of an acid activated montmorillonite clay with both acid and base ( $-\text{SO}_3\text{H}$  and  $-\text{NH}_2$ ) functional groups. FTIR,  $^{29}\text{Si}$  and  $^{13}\text{C}$  CP MAS NMR spectroscopy studies confirm the grafting of the organic functional moieties. These materials were also extensively characterized by various other characterization techniques like XRD,  $\text{N}_2$  adsorption–desorption analysis, XPS, FE-SEM, TEM, etc. This multi-functionalized material was investigated as a heterogeneous catalyst for one-pot deacetalization–nitroaldol (Henry) reaction giving a 99.2% product yield in just 2 h. This material also showed outstanding adsorption capacity for the heavy metal cations and can be utilized as a potential candidate for the remediation of contaminated water. This material is potent enough to carry out the Henry reaction as well as adsorption for many runs without any significant loss of its activity.

Received 3rd January 2014  
Accepted 3rd March 2014

DOI: 10.1039/c4ta00042k

[www.rsc.org/MaterialsA](http://www.rsc.org/MaterialsA)

## 1. Introduction

Clays are perfectly ideal support materials in heterogeneous catalysis, since they are naturally abundant, cheap, non-hazardous, chemically versatile, and recyclable.<sup>1</sup> Apart from their role in heterogeneous catalysis, clays are also excellent adsorbents for the removal of heavy metals which are harmful to the flora and fauna, and showed their efficacy in water pollution abatement.<sup>2</sup> Among wide varieties of clay, montmorillonite has been highlighted prominently in the literature for organic syntheses as well as adsorption.

Montmorillonite is a 2 : 1 layered silicate, where one alumina octahedral layer is sandwiched between two tetrahedral silica layers. The structural defects in the Si–O tetrahedral sheet and the layer edges with “broken” bonds in montmorillonite are similar to the Si atom environment in silica, and combine with organic moieties to form organo–inorganic hybrid materials.<sup>3–5</sup> Commercially available K10 is an acid activated montmorillonite. During its preparation, the  $\text{Al}^{3+}$  ions from the octahedral layers get leached out because of acid treatment on natural clay, creating mesopores, thereby resulting in a high surface area material. At the same time the

interlayer cations get replaced with the protons. The protons substituting the interlayer cations and the leached hydrated alumina occupying the cation exchange sites result in an improved acidity in K10 montmorillonite (K10-MMT).<sup>6,7</sup> During acid treatment, de-alumination causes formation of additional hydroxyl groups in the clay skeleton, which can easily graft the organic moieties to form organo–inorganic hybrid materials.

In our previous studies, we have reported many organically functionalized supports in heterogeneous catalysis for organic reactions.<sup>3–5,8–11</sup> However, in heterogeneous catalysis, multi-functionalization of a given solid support with both acidic and basic groups is of extreme interest for co-operative catalysis in one-pot reactions, which saves energy, time and the amount of solvents used. For instance, the combination of weak and strong acids with various organic bases on solid supports was investigated and synergistic catalytic enhancements were observed by various groups in the past.<sup>12–15</sup>

As a part of our on-going research on functionalization of montmorillonite, in this work, we have reported a bifunctional montmorillonite ( $\text{SO}_3\text{H}$ -APTES@K10-MMT), where the surface hydroxyl groups of montmorillonite are grafted with binary acid–base functionalities, such as sulfonic acid ( $-\text{SO}_3\text{H}$ ) and amine ( $-\text{NH}_2$ ) groups. These acid–base functionalities on an acidic clay support acted as bifunctional catalysts in one-pot Henry reaction. The Henry reaction is one of the most useful carbon–carbon bond forming reactions and can be catalyzed by organic and inorganic bases. There are a few literature reports on functionalized mesoporous materials toward the nitroaldol reaction. But a one-pot deacetalization–nitroaldol reaction is very rare.

<sup>a</sup>Colloids and Materials Chemistry Department, CSIR-Institute of Minerals and Materials Technology, Bhubaneswar-751013, Odisha, India. E-mail: [paridakulamani@yahoo.com](mailto:paridakulamani@yahoo.com); Fax: +91 674 2581637; Tel: +91 674 2581636 ext. 9425

<sup>b</sup>Academy of Scientific and Innovative Research (AcSIR), Anusandhan Bhawan, 2 Rafi Marg, New Delhi-110 001, India

<sup>c</sup>Central Characterization Cell, CSIR-Institute of Minerals and Materials Technology, Bhubaneswar-751013, Odisha, India

Apart from the one-pot reaction sequences, the functionalized supports also help in the remediation of global and environmental problems such as water pollution. Heavy metals are the chief pollutants released from chemical manufacturing, mining, extractive metallurgy, painting and coating, nuclear and other industries, *etc.* These metals create a harmful effect on the flora and fauna of streams and lakes and also weaken the mental and neurological functions. Therefore, a great deal of attention has been given by several research groups for the removal of heavy metals from natural and industrial wastewater. Out of a variety of methods, till now adsorption is the especially popular and frequently used technique due to its cleanliness, low cost as well as superior efficiency.

In this paper, we described a simple and efficient method of synthesizing a multi-functionalized material possessing amine and sulfonic acid groups on a K10-MMT clay surface. This system has been investigated for one-pot Henry reaction as well as removal of heavy metal ions by adsorption.

## 2. Experimental

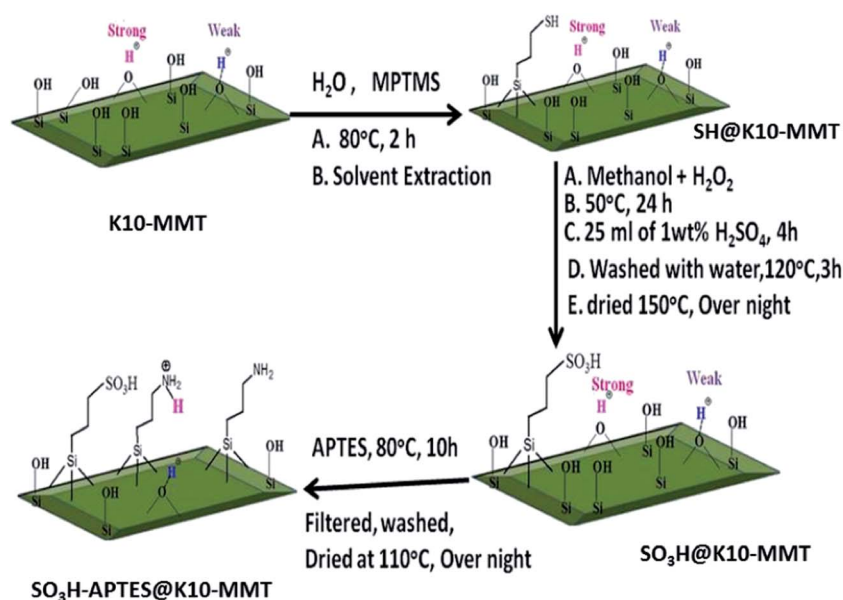
### 2.1 Synthesis of the catalyst

1 g K10-MMT in 30 ml water was stirred for 30 minutes at room temperature, and then 0.37 ml mercaptopropyl trimethoxysilane (MPTMS) was added into it. Finally, the mixture was stirred at 80 °C for two hours to give thiol functionalized K10-MMT (SH@K10-MMT). After solvent extraction, the thiol group was oxidized to sulfonic acid by using H<sub>2</sub>O<sub>2</sub> in the presence of methanol at 50 °C for 24 h (2.38 ml of 30% H<sub>2</sub>O<sub>2</sub> in 7.14 ml methanol for 1 g of SH@K10-MMT). The oxidized material was suspended in 25 ml of 1 wt% H<sub>2</sub>SO<sub>4</sub> for 4 h, washed with water, and then dried in a vacuum (120 °C, 3 h). The sample was designated as SO<sub>3</sub>H@K10-MMT. After the sample was dried overnight at 150 °C to remove the physisorbed water, 1 g

SO<sub>3</sub>H@K10-MMT was stirred vigorously in 80 ml dry toluene containing 0.84 mmol 3-aminopropyltriethoxysilane (APTES) at 80 °C for 10 h. The solution was filtered and the resultant solid was washed with dichloromethane, followed by ethanol. The solid material was allowed to dry under ambient conditions, resulting in SO<sub>3</sub>H-APTES@K10-MMT. Preparation of the multi-functionalized catalyst SO<sub>3</sub>H-APTES@K10-MMT is shown in Scheme 1.

### 2.2 Characterization techniques

PXRD patterns of the powdered samples were taken in the 2 $\theta$  range of 10 to 80° at a rate of 2° min<sup>-1</sup> in steps of 0.01° (Rigaku Miniflex set at 30 kV and 15 mA) using Cu K $\alpha$  radiation. The FTIR spectra of the samples were recorded using a Varian 800-FTIR in a KBr matrix in the range of 4000–400 cm<sup>-1</sup>. Solid state <sup>13</sup>C and <sup>29</sup>Si CP MAS NMR spectra were recorded on an AV300 NMR spectrometer. The BET surface area and total pore volume of all the samples were determined by the multipoint N<sub>2</sub> adsorption–desorption method at liquid N<sub>2</sub> temperature (–196 °C) using an ASAP 2020 (Micromeritics). Prior to analyses, all the samples were degassed at 300 °C and 10<sup>-6</sup> Torr pressure for 5 h to evacuate the physisorbed moisture. The electronic structure aspects of the samples were investigated by X-ray photoelectron spectroscopy using KRATOS apparatus with Mg, Al and Cu K $\alpha$  as X-ray sources. FE-SEM was performed with a ZEISS 55 microscope. The transmission electron micrographs of the samples were recorded using a microscope (FEI, TECNAI G<sup>2</sup> 20, TWIN) operating at 200 kV. The atomic absorption spectrometric analysis was carried out with a Perkin-Elmer Analysis 300 instrument using an acetylene (C<sub>2</sub>H<sub>2</sub>) flame. The back titration method was used to measure the amount of acidic and basic centers of the SO<sub>3</sub>H-APTES@K10-MMT.<sup>16</sup> About 0.1 g of the sample was added to a conical flask, and then 10 ml 0.01 M HCl (NaOH) solution was added. The mixture was stirred at



Scheme 1 Preparation of SO<sub>3</sub>H-APTES@K10-MMT.

room temperature for half an hour; then, the mixture was filtered and rinsed repeatedly for four times with 25 ml distilled water. The resulting filtrate was titrated with 0.01 M NaOH (HCl) solution using phenolphthalein as an indicator.

### 2.3 One-pot Henry reaction

The one-pot Henry reaction was carried out using the prepared samples. In a typical experiment, catalyst (0.05 g), benzaldehyde dimethylacetal (1.0 mmol) and nitromethane (5 ml) were placed in a 50 ml two necked round bottom flask, fitted with a reflux condenser. The resulting mixture was vigorously stirred at 90 °C under nitrogen for 2 h with a magnetic stirrer. The products were analyzed with a gas chromatograph (GC).

### 2.4 Adsorption studies

Stock solutions of Hg, Cd, and Pb cations were prepared by dissolving the corresponding metal salts in distilled water. For the adsorption measurements of heavy metals, 0.02 g of the sample was added into a 20 ml solution of known concentration (ppb) of the analyzing ions such as Hg<sup>2+</sup>, Cd<sup>2+</sup> and Pb<sup>2+</sup>. Then this solution was allowed to stir for 3 h, followed by filtration. The concentration of the cations in the initial solution and final filtrate was estimated by utilizing atomic absorption spectroscopy (AAS), using standard solutions to calibrate the instrument. The percentage removal of heavy metal cations was calculated according to the following equation:

$$R = \frac{C_0 - C_f}{C_0} \times 100\% \quad (1)$$

The adsorption amounts ( $Q_e$ ) were calculated according to the following equation:

$$Q_e = \frac{V(C_0 - C_f)}{M} \quad (2)$$

The solid/water distribution ratios ( $K_d$ ) of metals were calculated by the following equation:

$$K_d = \frac{C_0 - C_f}{C_f} \times \frac{V}{M} \quad (3)$$

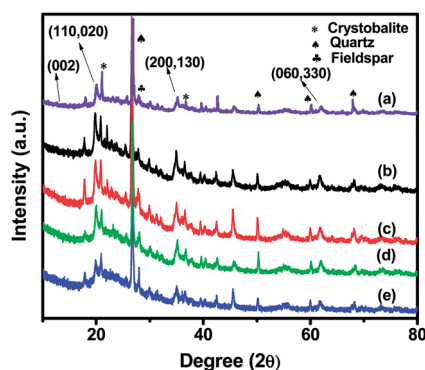


Fig. 1 Broad angle XRD spectra of K10-MMT (a), SH@K10-MMT (b), SO<sub>3</sub>H@K10-MMT (c), and the reused catalyst SO<sub>3</sub>H-APTES@K10-MMT (d) of the Henry reaction.

where  $C_0$  and  $C_f$  are the initial and final (equilibrium) concentrations of the metal ions in solution (mg l<sup>-1</sup>),  $V$  is the solution volume in ml, and  $M$  is the mass of sorbent in g.

**2.4.1 Desorption and reuse of the adsorbents.** The reusability of the adsorbents for metal ion adsorption was determined. Measurements were repeated for many consecutive adsorption-desorption cycles using the same adsorbent. Desorption of metal ions was measured in a 10 mM HCl-HNO<sub>3</sub> solution. The adsorbed metal ions on the adsorbents were placed in the desorption medium and stirred for 1 h at room temperature. The final metal ion concentration in the aqueous phase was determined by using AAS. The desorption ratio was calculated from the amount of metal ion adsorbed by the adsorbents and the final metal ion concentration in the desorption medium by the following equation

$$\text{Desorption ratio (\%)} = \frac{\text{(amount of metal ions desorbed to the elution medium)} \times 100}{\text{(amount of metal ions adsorbed onto adsorbents)}}$$

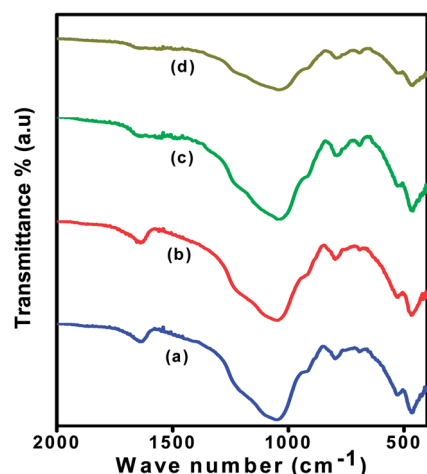
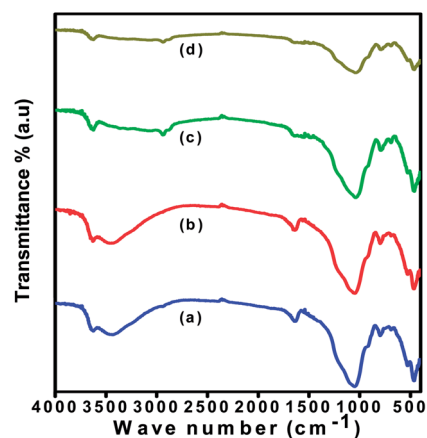


Fig. 2 (A) FT-IR spectra of SH@K10-MMT (a), SO<sub>3</sub>H@K10-MMT (b), SO<sub>3</sub>H-APTES@K10-MMT (c) and the reused catalyst SO<sub>3</sub>H-APTES@K10-MMT (d) of the Henry reaction. (B) FT-IR spectra of SH@K10-MMT (a), SO<sub>3</sub>H@K10-MMT (b), SO<sub>3</sub>H-APTES@K10-MMT (c) and the reused catalyst SO<sub>3</sub>H-APTES@K10-MMT (d) of the Henry reaction.

### 3. Results and discussion

#### 3.1 XRD

The diffraction patterns of K10-MMT are indicative of a main contribution of the mineral family corresponding to a typical smectite “montmorillonite” (Fig. 1). Along with *hkl* and two dimensional *hk* reflections, a number of peaks can also be seen due to many impurities like quartz, cristobalite and feldspar. The similar nature in the spectrum of all the samples suggests no structural change in the clay matrix upon grafting of the organic functional moieties.

#### 3.2 FTIR spectra

The FTIR spectra of various samples are shown in Fig. 2A. The FTIR spectra of all samples show a broad band in the region of  $3410\text{ cm}^{-1}$ , due to asymmetric stretching of the  $\text{-OH}$  group and two bands at  $1621$  and  $1386\text{ cm}^{-1}$ , which are due to bending vibrations of  $\text{-(H-O-H)-}$  and  $\text{-(O-H-O)-}$  bonds. The peak at  $1032\text{ cm}^{-1}$  is assignable to the asymmetric stretching vibration of  $\text{S=O}$  bands and  $1125\text{ cm}^{-1}$  to the symmetric vibration of  $\text{S=}$

O bands. As an outcome of introducing the sulfonic groups into the acidic clay, an absorption of  $610\text{ cm}^{-1}$  was observed, which is attributed to the bending vibration of  $\text{-OH}$  groups hydrogen bonded to  $\text{SO}_3\text{H}$  groups.<sup>17</sup>

The weak bands at  $2941\text{ cm}^{-1}$  and  $2879\text{ cm}^{-1}$  correspond to the asymmetric and symmetric  $\text{CH}_2$  stretch as evidenced from the literature (Fig. 2B).<sup>18,19</sup> However, the presence of amine moieties can be evidenced by the appearance of a relatively weak amide band ( $1536\text{ cm}^{-1}$ , N-H stretching). Since both the  $\text{CH}_2$  and  $\text{NH}_2$  groups are attached with the APTES skeleton, the above observations suggest the presence of APTES on the surface of K10-MMT. The spectra of the reused catalyst showed low intensity but the proximity in all the peaks with the original sample strongly supports the stability of the catalyst.

#### 3.3 NMR

Solid state  $^{29}\text{Si}$  CP-MAS NMR spectra provide information on the spectroscopic evidence on the presence of the desired organic functional groups on the clay surface as well as provide information on the coordination environments of silicon atoms

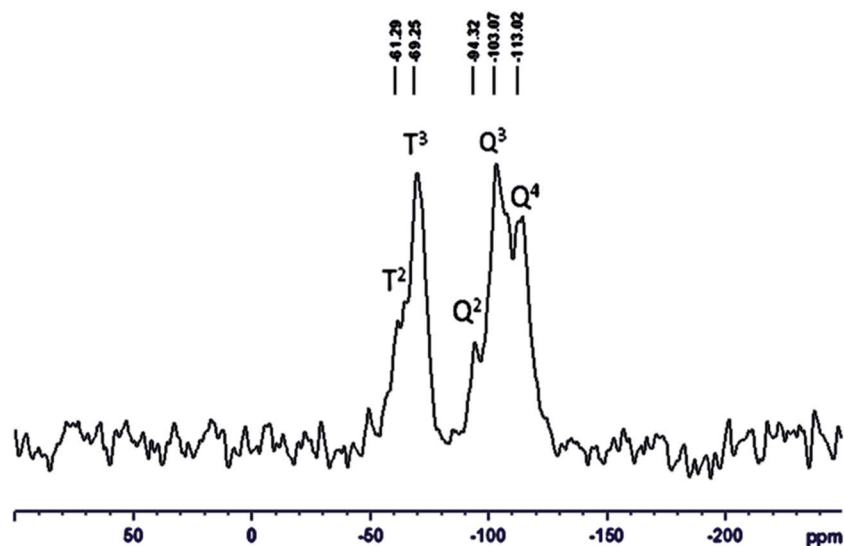


Fig. 3  $^{29}\text{Si}$  CP-MAS NMR spectra of  $\text{SO}_3\text{H-APTES@K10-MMT}$ .

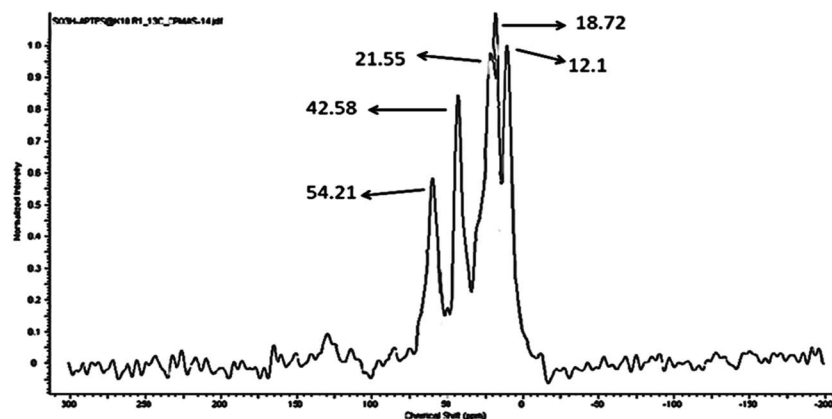


Fig. 4  $^{13}\text{C}$  CP-MAS NMR spectra of  $\text{SO}_3\text{H-APTES@K10-MMT}$ .

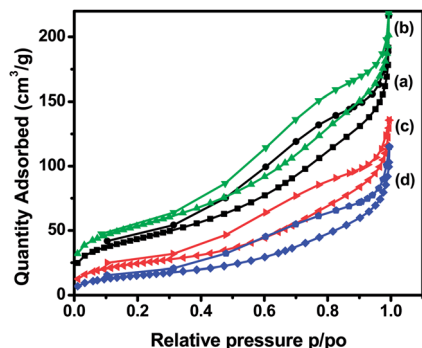


Fig. 5  $N_2$  adsorption-desorption spectra of SH@K10-MMT (a),  $SO_3H$ @K10-MMT (b),  $SO_3H$ -APTES@K10-MMT (c) and the reused catalyst  $SO_3H$ -APTES@K10-MMT (d) of the Henry reaction.

Table 1 Surface properties of various samples prepared

Catalyst	Surface area ( $m^2 g^{-1}$ )	Pore volume ( $cm^3 g^{-1}$ )
K10-MMT	241.41	0.41
SH@K10-MMT	201.34	0.36
$SO_3H$ @K10-MMT	200.98	0.36
$SO_3H$ -APTES@K10-MMT	154.54	0.32
$SO_3H$ -APTES@K10-MMT <sup>a</sup>	153.21	0.32

<sup>a</sup> Reused catalyst of the Henry reaction.

in the multi-functionalized clay materials. The solid state NMR spectrum of  $SO_3H$ -APTES@K10-MMT (Fig. 3) shows peaks for  $Q^4(0Al)$  units of amorphous silica with a three-dimensional

cross-linked framework,  $Q^3(0Al)$  due to poor-ordering of the framework without the possibility of cross-linking,  $Q^3(1Al)$  and  $Q^4(1Al)$  Si atoms with respective co-ordination  $Si(OSi)_4$ ,  $Si(OSi)_3(OH)$ ,  $Si(OSi)_2(OAl)OH$ , and  $Si(OSi)_3(OAl)$  in the clay framework at  $-113$  ppm,  $-103$  ppm and  $-94$  ppm, respectively. Apart from those peaks, two downfield peaks at  $-69$  ppm and  $-61$  ppm can be observed corresponding to  $T^3$  and  $T^2$  respectively, where  $T^n = [RSi(OEt)_n(OSi)_{3-n}]$ . This confirms a strong covalent linkage of the functional groups on the clay surface.

The presence of organic acid-base functional groups was further verified by solid-state  $^{13}C$  CP MAS NMR spectroscopy. The solid-state  $^{13}C$  CP MAS NMR spectrum of the  $SO_3H$ -APTES@K10-MMT sample is shown in Fig. 4. As shown in the  $^{13}C$  CP MAS NMR spectra of  $SO_3H$ -APTES@K10-MMT, three peaks at 12.1, 18.72 and 54.21 ppm correspond to the carbons of  $Si-CH_2-CH_2-CH_2-SO_3H$  from left to right, respectively<sup>20</sup> indicating the appearance of an acid functionality. On the other hand, the three distinct peaks at 11.2, 21.55 and 42.58 ppm represent the carbons of  $Si-CH_2-CH_2-CH_2-NH_2$  from left to right, respectively<sup>21</sup> proving the existence of a base functionality.

### 3.4 $N_2$ adsorption-desorption study

The nitrogen adsorption-desorption isotherms of various materials are shown in Fig. 5. All the prepared samples were examined by this technique and the main results are summarized in Table 1. All the samples behave according to the same trend. As can be seen from the curve, all of them belong to type IV isotherm according to BDDT (Brunauer-Deming-Deming-Teller) classification.<sup>22</sup> They show a large hysteresis loop illustrative of a mesoporous structure, in accordance with our

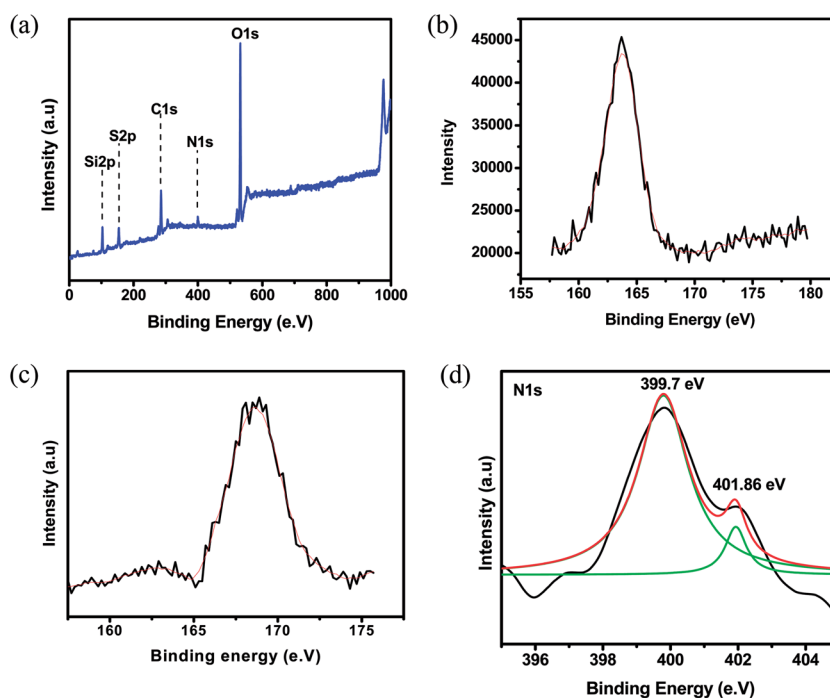


Fig. 6 (a) XPS spectrum of  $SO_3H$ -APTES@K10-MMT. (b) S  $2p_{3/2}$  of SH@K10-MMT. (c) S  $2p_{3/2}$  of  $SO_3H$ -APTES@K10-MMT. (d) N 1s of  $SO_3H$ -APTES@K10-MMT.

previous reports on acid activated montmorillonite based materials.<sup>23</sup> After the grafting of organic functional groups, a substantial decrease in nitrogen uptake is reflected in a decrease in surface area and pore volume of the sample (Table 1). Such a decrease in these parameters could be attributed to the space occupied by the grafting agents.

### 3.5 XPS

The acid–base bi-functionalization on K10-MMT was also established through the XPS study. The total survey scans of  $\text{SO}_3\text{H-APTES@K10-MMT}$  are shown in Fig. 6a. This reveals the

existence of elements like S, N and C, along with the elements of the neat clay.

The XPS spectrum of  $\text{SH-APTES@K10-MMT}$  exhibits a peak with a binding energy of 166 eV for the S 2p electron of  $-\text{SH}$  (Fig. 6b). A main peak with a binding energy of 168.8 eV was detected in the XPS spectrum of  $\text{SO}_3\text{H-APTES@K10-MMT}$ . The binding energy of 168.8 eV is close to the expected values for sulfonic acid (169 eV) and hence can be assigned to the binding energy for the S 2p electron of the  $-\text{SO}_3\text{H}$  species (Fig. 6c).<sup>24</sup> The above results confirm that the  $-\text{SH}$  group could be successfully transformed to  $-\text{SO}_3\text{H}$  by using  $\text{H}_2\text{O}_2$  at 50 °C.

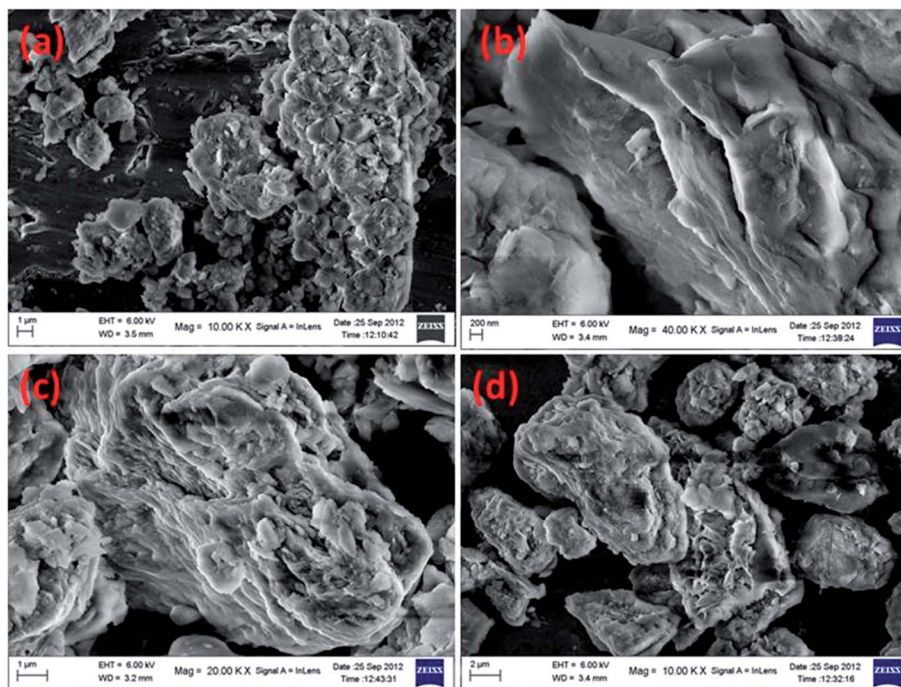


Fig. 7 FESEM spectra of  $\text{SH@K10-MMT}$  (a),  $\text{SO}_3\text{H@K10-MMT}$  (b),  $\text{SO}_3\text{H-APTES@K10-MMT}$  (c) and the reused catalyst  $\text{SO}_3\text{H-APTES@K10-MMT}$  of the Henry reaction (d).

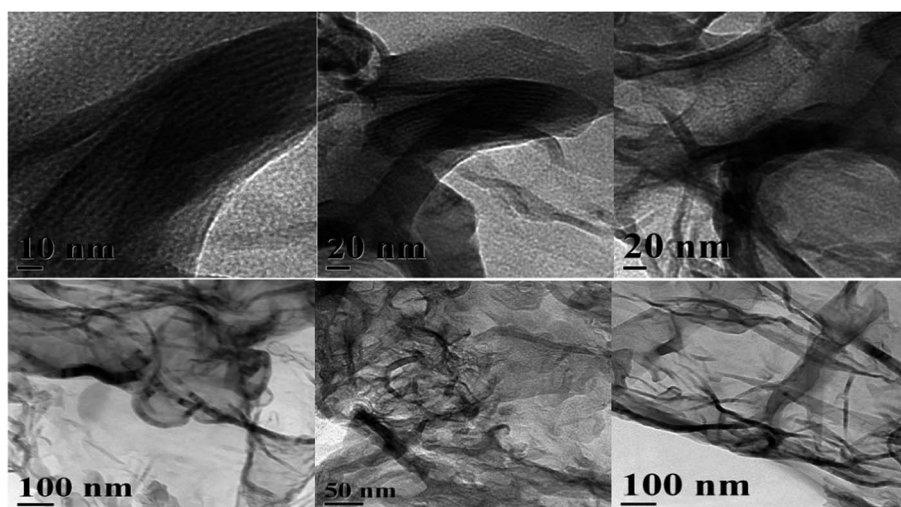


Fig. 8 TEM image of  $\text{SO}_3\text{H-APTES@K10-MMT}$ .

In N 1s spectra of SO<sub>3</sub>H-APTES@K10-MMT, two peaks can be observed at 399.7 eV and 401.62 eV (Fig. 6d). The standard binding energy for the free amine group (–NH<sub>2</sub>) falls in the region of 399–401 eV, while the protonated amine (–NH<sub>3</sub><sup>+</sup>) has a higher binding energy of 1.0 eV above the free amine. So, the binding energy at 399.7 eV is assigned to the –NH<sub>2</sub> while the binding energy at 401.86 eV is attributed to –NH<sub>3</sub><sup>+</sup> groups.

### 3.6 FESEM and TEM

Field emission scanning electron micrographs of various materials are shown in Fig. 7. Generally K10-MMT is a multi-layered material consisting of many parallel arrays of broken plates, which upon functionalization shows no change. The retention of montmorillonite sheets after functionalization could also be observed from the TEM micrographs (Fig. 8). The TEM images of the SO<sub>3</sub>H-APTES@K10-MMT show randomly oriented crumpled sheets.

### 3.7 Quantification of acidic and basic sites

Quantification of the acidic and basic centers on SO<sub>3</sub>H-APTES@K10-MMT was performed using the back titration method. Those results confirm the coexistence of both the acidic and basic sites in the catalysts. The amount of base centers in SO<sub>3</sub>H-APTES@K10-MMT is 0.52 mmol g<sup>–1</sup>, whereas that of acid centers is 0.64 mmol g<sup>–1</sup>.

## 4. Catalytic applications

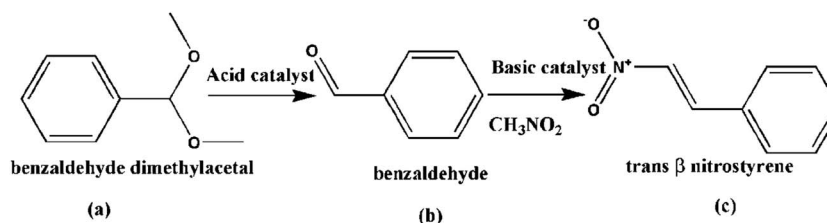
### 4.1 Liquid phase one-pot Henry reaction

In order to test the compatibility of these acid–base bi-functional catalysts in catalyzing the one-pot cascade reactions, different prepared samples were applied to the chemical transformation of benzaldehyde dimethylacetal (compound 1) to benzaldehyde

(compound 2), which was then converted to *trans*-β nitrostyrene (compound 3). From Table 2, it can be observed that there is no conversion and yield of products in the absence of catalyst. In the presence of K10-MMT, the conversion of compound 1 is less but there is no conversion of compound 2 to compound 3. SO<sub>3</sub>H-APTES@K10-MMT converted benzaldehyde dimethylacetal to the desired product in quantitative yield after a reaction time of 2 h. In particular, during the reaction process, almost no intermediate species were detected (Table 2, entries 3–5 with different reaction times), showing high activity and excellent selectivity of the bi-functional catalyst. In the presence of SO<sub>3</sub>H-APTES@K10-MMT, the conversion and the yield% increase because in the first step both the –SO<sub>3</sub>H group and protonated amine group (–NH<sub>3</sub><sup>+</sup>) activate the acid catalyzed reactions, then the basic amine group (–NH<sub>2</sub>) activates the base catalyzed reaction. In addition, the efficient acid/base active sites might increase due to protection of amino groups from the interaction between acid and base.<sup>25</sup> In sharp contrast, monofunctional catalysts, APTES@K10-MMT or SO<sub>3</sub>H@K10-MMT (Table 2, entries 6 and 7), did not produce the desired target product, although both of them were able to catalyze the first step reaction to a small extent. Difference in catalytic activity can also be observed with the variation of reaction time. The conversion as well as the final product yield increased on changing the reaction time from 1 h to 2 h. However after 2 h, the conversion and product yield remained fairly constant (Table 2, entries 3–5).

In a final set of experiments, we investigated the stability of the catalyst, because it is crucial to confirm that high-activity catalysts can be reused. The catalyst was recovered by centrifugation and directly reused in the next run. Results showed that the catalyst could be reused 3 times without a significant loss of catalytic activity. The nature and yield of the final products were compared with those of the original run. The results are shown in Fig. 9.

Table 2 Effect of various catalysts on the one pot reaction<sup>a</sup>



Entries	Catalyst	Conversion of a (%)	Yield of b (%)	Yield of c (%)
1	Without catalyst	0	0	0
2	K10-MMT	5	5	0
3	SO <sub>3</sub> H-APTES@K10-MMT	99	0.8	99.2
4	SO <sub>3</sub> H-APTES@K10-MMT <sup>b</sup>	78	0.3	82.5
5	SO <sub>3</sub> H-APTES@K10-MMT <sup>c</sup>	99	0.9	99.4
6	APTES@K10-MMT	6	4	2
7	SO <sub>3</sub> H@K10-MMT	50	50	0
8	SH@K10-MMT	6	5	0

<sup>a</sup> Reaction conditions: catalyst (0.05 g), reaction time 2 h, benzaldehyde dimethylacetal (1.0 mmol) and nitromethane (5 ml), temperature: 90 °C.

<sup>b</sup> Reaction time 1 h. <sup>c</sup> Reaction time 3 h.

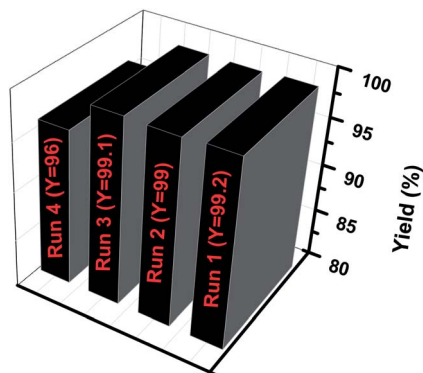


Fig. 9 Results of recycling tests for the one-pot Henry reaction. Y = yield%.

FT-IR spectra of the fresh as well as the regenerated catalysts are shown in Fig. 2(A and B). It can be seen that though there is a decrease in intensity, the spectra of the reused catalysts are quite similar to those of the fresh ones. This confirms the retention of the catalyst structure. Also XRD and N<sub>2</sub> adsorption-desorption studies of the reused catalysts confirmed that there is no change in the catalyst structure as compared to the fresh catalyst.

#### 4.2 Adsorption studies towards heavy metals

The adsorption performances of K10-MMT and SO<sub>3</sub>H-APTES@K10-MMT are shown in Table 3. The multi-functionalized

Table 3 Results of adsorption performances of various samples towards different metal ions

Sample	Solution (20 ml)	Cation content (ppb)		Cation removal efficiency R (%)	Distribution co-efficient (K <sub>d</sub> ) (ml g <sup>-1</sup> )
		Before	After		
1. K10-MMT	Hg <sup>2+</sup>	200	15.2986	92.35	1.207 × 10 <sup>4</sup>
	Cd <sup>2+</sup>	200	44	78.0	3.545 × 10 <sup>3</sup>
	Pb <sup>2+</sup>	200	30	85.0	5.67 × 10 <sup>3</sup>
2. SH@K10-MMT	Hg <sup>2+</sup>	200	11	94.5	1.7 × 10 <sup>4</sup>
	Cd <sup>2+</sup>	200	31.1982	84.4	5.41 × 10 <sup>3</sup>
	Pb <sup>2+</sup>	200	21	89.5	8.52 × 10 <sup>3</sup>
3. SO <sub>3</sub> H@K10-MMT	Hg <sup>2+</sup>	200	10.3217	94.83	1.83 × 10 <sup>4</sup>
	Cd <sup>2+</sup>	200	29	85.5	5.89 × 10 <sup>3</sup>
	Pb <sup>2+</sup>	200	19	90.5	9.52 × 10 <sup>3</sup>
4. SO <sub>3</sub> H-APTES@K10-MMT	Hg <sup>2+</sup>	200	6.1947	96.9	3.128 × 10 <sup>4</sup>
	Cd <sup>2+</sup>	200	18	91.0	1.011 × 10 <sup>4</sup>
	Pb <sup>2+</sup>	200	15	92.5	1.233 × 10 <sup>4</sup>

Table 4 A comparative study of adsorption of different heavy metal ions by different types of mesoporous materials

Entry	Sample	Metal cation	Distribution co-efficient K <sub>d</sub> (ml g <sup>-1</sup> )	Ref.
1	Aluminosilicate	Cd <sup>2+</sup>	7–1.2 × 10 <sup>3</sup>	26
2	LHMS-2	Hg <sup>2+</sup> and Cd <sup>2+</sup>	8.03 × 10 <sup>3</sup> and 6.47 × 10 <sup>3</sup>	27
3	Amine functionalized silica	Pd <sup>2+</sup>	1.49 × 10 <sup>2</sup> –3.31 × 10 <sup>4</sup>	28
4	NH <sub>2</sub> -MCM-41	Cd <sup>2+</sup>	7.2 × 10 <sup>2</sup>	29
5	Thioether	Hg <sup>2+</sup> and Pb <sup>2+</sup>	8.35–9.19 × 10 <sup>2</sup> and 7.5–34.48	30
6	SO <sub>3</sub> H-APTES@K10-MMT	Hg <sup>2+</sup> , Cd <sup>2+</sup> and Pb <sup>2+</sup>	3.128 × 10 <sup>4</sup> , 1.011 × 10 <sup>4</sup> and 1.233 × 10 <sup>4</sup>	Present work

K10-MMT materials exhibited a higher adsorption capacity for Hg<sup>2+</sup>, Cd<sup>2+</sup> and Pb<sup>2+</sup> than parent K10-MMT. The (–NH<sub>2</sub>) groups and (–SO<sub>3</sub>H) groups in the adsorbent provided the effective adsorption sites. Heavy metal ions have a preference for coordinating with (–SO<sub>3</sub>H) groups and (–NH<sub>2</sub>) groups that have more or less electronegative donor atoms and these have a strong coordination role with metal ions. Amines are known to be versatile ligands and when attached to the acid activated clay surface, they increased the ligand strength of the surface, thereby increasing the affinity of the sorbent material for metal ions, whereas the –SO<sub>3</sub>H group may function as an acid in combining with a metal atom by the replacement of hydrogen ions. The results shown in Table 3 prove that the (–SO<sub>3</sub>H) groups and (–NH<sub>2</sub>) groups in the adsorbent are the effective adsorption sites.

A comparative study of the adsorption of heavy metal cations by different classes of functionalized mesoporous materials is shown in Table 4.<sup>26–30</sup> From this comparison it is quite clear that the multifunctional materials prepared by us reported good adsorption ability for different heavy metal cations. Having good adsorption efficiencies for heavy metals the mesoporous SO<sub>3</sub>H-APTES@K10-MMT material can be employed as an adsorbent for the remediation of the contaminated water, which will have sustainable impact on controlling the environmental pollution.

**4.2.1 Desorption and reuse.** The desorption efficiencies of the adsorbed metal ions was found from 85–90%. The adsorption-desorption of metal ions were repeated for many times using the same adsorbent, *i.e.*, SO<sub>3</sub>H-APTES@K10-MMT. After 5 cycles, the cation removal efficiency for Hg<sup>2+</sup>, Cd<sup>2+</sup> and Pb<sup>2+</sup> was found to be 94.1, 89.2 and 91.0% respectively, after which it decreased significantly. One probable cause of decrease in the adsorption capacity after repetitive use of the adsorbent for five cycles could be the negative effects of the desorbing agents on the functional moieties. The regeneration of the adsorbents shows that the process of adsorption-desorption is a reversible one and the adsorbents can be used repetitively for the removal of metal ions from aqueous solution.

## 5. Conclusions

A multi-functionalized catalyst that possesses the ability to act as a base and an acid has been synthesized by supporting APTES and MPTMS on the surface of K10-MMT. The catalyst was effective enough for the one pot Henry reaction, which involves two main reactions: (1) benzaldehyde dimethylacetal-to-benzaldehyde and (2) benzaldehyde-to-*trans*-β-nitrostyrene, and

each reaction needed an acid and a base catalyst respectively. As a result of the synergistic effect of the acid–base co-operative catalysis, all the two steps could be accomplished in a single pot with excellent activity, which were better than the individually grafted acid and base functional moieties on the clay surface. The investigation revealed that the one-pot Henry reaction requires a synergistic co-operative effect of both an acid and a base, which was provided by SO<sub>3</sub>H-APTES@K10-MMT. Most importantly, the catalyst was reusable, which is an important step towards simple systems with the potential for commercial exploitation of heterogeneous catalysts in one-pot reactions. Apart from its ability to act as an effective bi-functional catalyst in the one-pot Henry reaction, it was also potent enough to adsorb many heavy metal cations, due to the presence of S and N atoms in the functional groups helping in water pollution abatement. Studies on synthesis of such multi-functionalized catalysts for employment in many other one-pot reaction sequences as well as treating them as the effective adsorbents for water pollution remediation are underway in our laboratory.

## Acknowledgements

The authors are extremely thankful to Professor B. K. Mishra, Director, CSIR-IMMT, Bhubaneswar-751013, Odisha, India, for his constant encouragement and permission to publish this work. GBBV and SKR are obliged to CSIR for a senior research fellowship.

## References

- 1 A. Vaccari, *Catal. Today*, 1998, **41**, 53.
- 2 S. Sen Gupta and K. G. Bhattacharyya, *Phys. Chem. Chem. Phys.*, 2012, **14**, 6698.
- 3 G. B. B. Varadwaj, S. Rana and K. M. Parida, *Dalton Trans.*, 2013, **42**, 5122.
- 4 G. B. B. Varadwaj, S. Rana and K. M. Parida, *RSC Adv.*, 2013, **3**, 7570.
- 5 G. B. B. Varadwaj, S. Rana and K. M. Parida, *J. Phys. Chem. C*, 2014, **118**, 1640.
- 6 I. Tkac, P. Komadel and D. Muller, *Clay Miner.*, 1994, **29**, 11.
- 7 C. Cativiela, J. M. Fraile, J. I. Garcia, J. A. Mayoral, F. Figueras, L. C. de Menorval and P. J. Alonso, *J. Catal.*, 1992, **137**, 394.
- 8 K. M. Parida and D. Rath, *J. Mol. Catal. A: Chem.*, 2009, **310**, 93.
- 9 K. M. Parida, S. Mallick, P. C. Sahoo and S. Rana, *Appl. Catal., A*, 2010, **381**, 226.
- 10 S. Rana, S. Mallick and K. M. Parida, *Ind. Eng. Chem. Res.*, 2011, **50**, 2055.
- 11 S. Mallick, S. Rana and K. M. Parida, *Dalton Trans.*, 2011, **40**, 9169.
- 12 B. Voit, *Angew. Chem., Int. Ed.*, 2006, **45**, 4238.
- 13 H. Groger, *Chem. – Eur. J.*, 2001, **7**, 5246.
- 14 F. Gelman, J. Blum and D. Avnir, *J. Am. Chem. Soc.*, 2000, **122**, 11999.
- 15 J. D. Bass, A. Solovyov, A. J. Pascal and A. Katz, *J. Am. Chem. Soc.*, 2006, **128**, 3737.
- 16 X. Yu, Y. Zou, S. Wu, H. Liu, J. Guan and Q. Kan, *Mater. Res. Bull.*, 2011, **46**, 951.
- 17 G. D. Yadav and A. D. Murkute, *Adv. Synth. Catal.*, 2004, **346**, 389.
- 18 L. Valentini, M. Cardinali and J. M. Kenny, *Carbon*, 2010, **48**, 861.
- 19 D. G. Kurth and T. Bein, *Langmuir*, 1993, **9**, 2965.
- 20 B. Rac, A. Molnar, P. Forgo, M. Mohai and I. Bertoti, *J. Mol. Catal. A: Chem.*, 2006, **244**, 46.
- 21 H.-M. Kao, C.-H. Liao, A. Palani and Y.-C. Liao, *Microporous Mesoporous Mater.*, 2008, **113**, 212.
- 22 S. Brunauer, L. S. Demming, W. E. Demming and E. Teller, *J. Am. Chem. Soc.*, 1940, **62**, 1723.
- 23 T. Mishra and K. M. Parida, *J. Mater. Chem.*, 1997, **7**, 147.
- 24 H. Moulder, W. F. Stickle, P. E. Sobol and K. D. Bomben, in *Handbook of X-ray Photoelectron Spectroscopy*, ed. J. Chastain, 1992.
- 25 Y. Shao, H. Liu, X. Yu, J. Guan and Q. Kan, *Mater. Res. Bull.*, 2012, **47**, 768.
- 26 H. Sepehrian, S. J. Ahmadi, S. Waqif-Husain, H. Faghian and H. Alighanbari, *J. Hazard. Mater.*, 2010, **176**, 252.
- 27 D. Chandra, S. K. Das and A. Bhaumik, *Microporous Mesoporous Mater.*, 2010, **128**, 34.
- 28 H. Yang, R. Xu, X. Xue, F. Li and G. Li, *J. Hazard. Mater.*, 2008, **152**, 690.
- 29 K. F. Lam, K. L. Yeung and A. McKay, *Environ. Sci. Technol.*, 2007, **41**, 3329.
- 30 M. Teng, H. Wang, F. Li and B. Zhang, *J. Colloid Interface Sci.*, 2011, **355**, 23.